# Nonlinear earthquake capacity of slender old masonry structures prestressed with steel, FRP and NiTi SMA tendons

Adolfo Preciado [*1], Alejandro Ramírez-Gaytan [2a], Nayar Gutierrez [1b],
David Vargas [1c], Jose Manuel Falcon [1d] and Gil Ochoa [1e]

[1] *Departamento del Hábitat y Desarrollo Urbano, Instituto Tecnológico y de Estudios Superiores de Occidente (ITESO),
Periférico Sur Manuel Gómez Morín 8585, 45604 Tlaquepaque, Jalisco, México*
[2] *Departamento de Ciencias Computacionales, Centro Universitario de Ciencias Exactas e Ingeniería,
Universidad de Guadalajara (UdeG), Boulevard Marcelino García Barragán 1421, 44430 Guadalajara, Jalisco, México*

**Abstract.** This paper focuses on the seismic protection of slender old masonry structures by the implementation of prestressing devices at key locations. The devices are vertically and externally located inside the towers in order to be reversible and calibrated. An extensive parametric study on a selected slender tower is carried out based on more than 100 nonlinear static simulations aimed at investigating the impact of different parameters on the seismic performance: (i) different prestressing levels; (ii) shape memory alloy superelasticity and (iii) changes in prestressing-forces in all the stages of the analysis until failure and masonry toe crushing. The tendon materials under analysis are conventional prestressing steel, fiber-reinforced polymers of different fibers and shape memory alloys. The parametric study serves to select the most suitable prestressing device and optimal prestressing level able to dissipate more earthquake energy. The seismic energy dissipation is evaluated by comparing the structural capacity curves in original state and retrofitted.

**Keywords:** strong earthquakes; unreinforced masonry; slender structures; prestressing; steel; fiber reinforced polymers; shape memory alloys; nonlinear analysis

## 1. Introduction

Slender unreinforced masonry (URM) structures as minarets, light houses, medieval and bell towers (see Fig. 1) are extremely vulnerable to suffer strong damage or complete collapse under earthquake (EQ) conditions, even when subjected to seismic events of low to moderate intensity. These monuments were built following empirical rules to mainly withstand vertical loading induced by their self weight, disregarding the effect of horizontal inertia forces transmitted by EQs. This is due to the limitations in materials technology and knowledge about EQs and structural behavior in that time. Protection of cultural heritage is a topic of great concern among the scientific community. Assessing the seismic vulnerability of a historical building represents an extensive and time consuming work due to the complexity in geometry, materials and limitations of the resistant system as explained in the research works of Sepe *et al*. (2008), Barbieri *et al*. (2013), Foraboschi (2013), Preciado *et al*.

∗Corresponding author, Ph.D., Professor,
  E-mail: adolfopreciado@iteso.mx
[a] Ph.D.
[b] Ph.D.
[c] Ph.D.
[d] Ph.D.
[e] Ph.D. Student
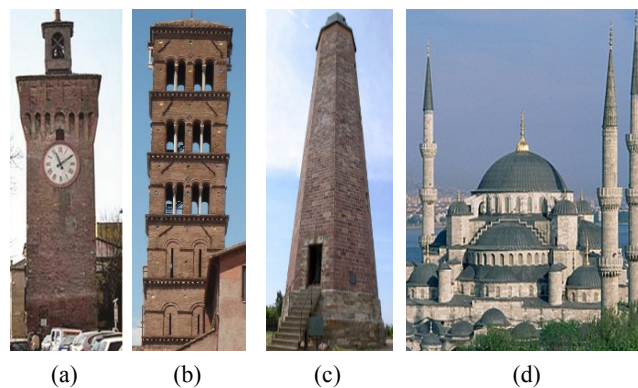
Fig. 1 Typical monumental slender URM structures; (a) medieval towers; (b) bell towers; (c) light houses and (d) minarets of Mosques

(2014) and Preciado and Orduña (2014).

The main difficulties on the seismic analysis and retrofitting of these structures arise from the high heterogeneity and heavy weight of masonry. The low tensile strength of masonry induces cracking since very low lateral loads and tends to separate the structure into macro-blocks that behave independently, presenting complex failure mechanisms. Degradation of masonry through time and long-term heavy loads are other important issues affecting the seismic behavior of slender URM structures. These tall and massive structures may present total failure even in static conditions when the concentration of stresses

overpasses the intrinsic compressive strength of the material as explained by Binda *et al.* (1992), Macchi (1993), GES (1993) and Binda (2008).

The present research is focused on high-rise masonry towers (taller than 30 m) with a failure mechanism governed by bending with relatively large displacements (some cases larger than 250 mm) at ultimate condition (peak point at the capacity curve). These large displacements and failure type are commonly observed in medieval or other masonry towers without belfries because of strong EQ motion. Bell-towers with large openings at belfries are more vulnerable to suffer a brittle collapse at this upper part by a concentration of shear stresses. Prestressing of masonry structures is not a recent strengthening technique as can be observed quite often in existing old masonry buildings and housing in Italy. The addition of different types of iron bars (anchorages and tighteners of the same material) was a common practice in past interventions. The prestressing effect was induced by heating the iron bar in order to expand the material and when returned to its normal temperature by contraction, the active prestressing force was activated by shortening effect. Through the history, the most frequent uses of old prestressing in ancient structures have been to tight and to connect walls in order to prevent overturning and to stabilize arches, vaults and domes that were damaged or identified as instable by opening or movement of their supports due to seismic forces. Moreover, the difficulties to generate a good connection between bars and the excessive concentration of stresses induced by the anchorage to the masonry could lead to local crushing at the contact surface (Preciado *et al.* 2015c). Another disadvantage was that the changes in prestressing forces by temperature, corrosion and material´s relaxation were not controlled nor monitored throughout the years. Foraboschi (2016a) studied the construction history of three well-known masonry domes located in Italy. In one of the historical domes, the author observed an external horizontal prestressing steel belt fixed onto the drum to solve the unstable behavior and safety conditions of the bare structure, demonstrating with this, that builders also considered prestressed masonry in the past.

In case of masonry domes, circumferential horizontal prestressing is an effective way of redirecting the horizontal forces transmitted by the heavy mass to the supports into vertical forces that prevent a state of instability by support's openings. Horizontal prestressing is more effective for avoiding an out-of-plane failure of domes and belfries of bell towers. Nowadays, prestressing structures take advantage of high resistance materials such as steel, reinforced polymers with the addition of fibers (e.g., glass, carbon, aramid, etc.) and nickel-titanium metal alloys with superelastic behavior. The ancient technique of heating the tendon is no longer used; instead, a prestressing jack applies the post-tension force directly to the tendon and anchorage. Horizontal prestressing with steel cables in tall masonry towers is not the best retrofitting solution, even when there is a reduction of damage, this may induce the development of localized tensile stresses at other locations affecting the overall seismic performance (e.g., Ganz 2002 and Stavroulaki *et al.* 2009). Conversely, the vertical post-

tensioning technique with tendons has proved to be more effective to increase the in-plane lateral load carrying capacity and ductility of masonry towers by providing tensile strength at key locations (e.g., Preciado *et al.* 2015a and 2017).

In this research, the seismic protection of slender URM structures is proposed by the implementation of vertical prestressing devices (PDs) at key locations. The devices are vertically located in the internal part of the tower by fixing them onto the wall surface in order to be reversible and without affecting the historical and architectonic value of the structure. Prestressing intends to improve the seismic performance by the application of a uniform overall distribution of compressive stresses to increase confinement, ductility, lateral strength and energy dissipation. An extensive parametric study on a selected URM tower is carried out based on more than 100 nonlinear static simulations aimed at investigating the impact of different parameters on the seismic performance. These parameters are related to the use of smart materials as the main component of tendons and anchorages against conventional prestressing steel.

Moreover, different prestressing levels (PLs) and changes in forces in all the stages of the analysis are also studied, especially at ultimate conditions where the structure may also fail by masonry crushing. The smart materials under analysis consist of fiber-reinforced polymers (FRPs) of different fibers such as aramid and carbon, as well as segments of shape memory alloys (SMA) combined with FRPs. The detailed parametric study also has the main objective of investigating the SMA superelasticity effect on the seismic performance of slender URM structures. SMA can undergo very large deformations in the loading and unloading cycles without permanent deformations, forming a loop interpreted as dissipation of energy. This superelastic material has found very interesting applications as seismic retrofitting of cultural heritage buildings; *e.g.* the façade of the Basilica of Saint Francis of Assisi in Umbria, Italy and the tower of the church of San Giorgio in Trignano, Italy investigated by Indirli *et al.* (2001) and Castellano (2001). However, in the last real application of SMAs, the retrofitting effectiveness was validated in qualitative terms by determining no damage on the tower after the occurrence of a considerable EQ, with no numerical simulations to support the effectiveness of the proposal.

The parametric study presented in this paper serves to select the most suitable PD and optimal PL able to dissipate more EQ energy. The seismic energy dissipation is evaluated by comparing the structural capacity curves in original state and retrofitted.

## 2. Description of the used masonry model

The homogenized masonry material model developed by Gambarotta and Lagomarsino (1997) is implemented in the nonlinear simulations. This model is capable to simulate the main failure modes and behavior of masonry structures in static and dynamic conditions. The suitability of the
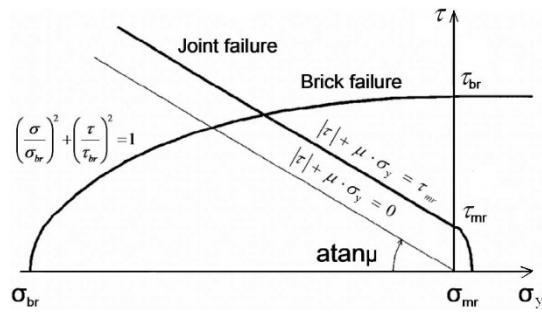
Fig. 2 Mortar joint and brick failure domains
(Gambarotta and Lagomarsino 1997)

Table 1 Summary of masonry inelastic parameters
for the material model

| Parameter | Value | Unit |
|---|---|---|
| $\sigma_m$: tensile strength for mortar | 0.25 | MPa |
| $\tau_m$: shear strength for mortar | 0.35 | MPa |
| $c_m$: shear inelastic compliance for mortar | 1 | - |
| $\beta_m$: softening coefficient for mortar | 0.7 | - |
| $\mu$: friction coefficient for mortar | 0.6 | - |
| $\sigma_M$: compressive strength of masonry | 3.5 | MPa |
| $\tau_b$: shear strength of units | 1.5 | MPa |
| $c_M$: inelastic compliance of masonry in compression | 1 | - |
| $\beta_M$: softening coefficient of masonry | 0.4 | - |

material model in masonry structures has been verified through numerical simulations (e.g., Calderini and Lagomarsino 2006, Urban 2007, Sperbeck 2009 and Preciado 2011) and against experimental results reported in literature (e.g., Van der Pluijm and Vermeltfoort 1991, Raijmakers and Vermeltfoort 1992 and Vermeltfoort and Raijmakers 1993). The continuum damage model is based on a micromechanical approach where masonry is assumed as a composite medium made up of an assembly of units connected by bed mortar joints. The contribution of head joints is not considered in the material model. The constitutive equations are obtained by homogenizing the composite medium and on the hypothesis of plane stress condition. The homogenized model is characterized by three yield surfaces determined by tensile failure and sliding of mortar joints considering the Coulomb friction law, as well as the compressive failure of units.

Fig. 2 shows the mortar joint and brick failure domains of the adopted constitutive masonry model. Besides the elastic parameters of masonry such as Young's modulus, Poisson's ratio and density, the material model requires nine nonlinear parameters as presented in Table 1. In summary, if tensile stresses act in mortar bed joints $\sigma_y \geq 0$, three damage mechanisms may become active: failure of units; sliding and failure of mortar bed joints. On the other hand, if mortar joints are under compressive stresses $\sigma_y < 0$, then both damage mechanisms of units and mortar are activated.

The model is able to describe stiffness and strength degradation for structures monotonically loaded in-plane and out-of-plane as well as the hysteretic response by cyclic loading. Energy dissipation is possible through activated frictional mechanisms. Another important feature of this accurate material model is that it is able to consider the evolution of damage in the units and mortar bed joints by especial damage parameters that are helpful to predict the structural failure mechanisms. The damage distribution of structures subjected to nonlinear analyses through FEM simulations is represented by inelastic plastic strain contours. Since stresses (localized tension and compression) in all the stages of the numerical simulation tend to redistribute and change, the inelastic deformation are permanent and represent an approximated approach for generalized damaged parts (cracking) and areas of concentration of stresses at the structure. The summary of masonry material parameters are described in Table 1.

## 3. Reversible retrofitting of slender URM structures

The most effective technique to convert URM intoreinforced masonry is to epoxy bond Fiber Reinforced Polymer (FRP) strips onto the external surface of the masonry (Foraboschi 2015). Retrofitting of masonry structures by the use of bonded FRPs has been also studied by Ascione *et al*. (2005), D'Ambrisi *et al*. (2013a, b), Muciaccia and Biolzi (2012) and Fedele *et al*. (2014). The use of carbon FRPs (CFRP) strips is being highly used in existing reinforced concrete structures for enhancing shear and bending resistance (Panjehpour *et al*. 2014, Bansal *et al*. 2016 and Hadji *et al*. 2016), as well as enhancing the flexural behavior of existing steel structures (Park and Yoo 2015). Foraboschi (2015) explains that FRP strips may suffer from low crack growth; therefore, new strategies to bond the strips onto the masonry surface must be developed. These methods have been studied more in detail by Foraboschi and Vanin (2013) and Foraboschi (2016b). Since historical buildings must be retrofitted with reversible techniques to avoid affecting the architectonic and historic value, no plaster and FRP strips may be fixed onto the bare-masonry surface. Moreover, FRP strips bonded onto the masonry surface in some cases is not the best solution; therefore, the need of another technique such as prestressed tendons is suggested to be used for the seismic protection of cultural heritage. Prestressing of masonry has shown to improve ductility and strength successfully as explained by Ganz (1990 and 2002), Indirli *et al*. (2001), Castellano (2001), Sperbeck (2009) and Preciado (2011).

External or internal (both fixed onto the bare-surface of the walls) prestressing is commonly applied at key identified points of the structure in the seismic vulnerability assessment stage. This technique is in compliance with the demand for architectural conservation and may be located unbonded in order to be fully removable. The no-bonding condition allows further calibration and control of changes in prestressing force (PF) by material relaxation. Some of the few cases reported in literature regarding the seismic protection of slender masonry structures are mainly focused on bell towers (Ganz 2002, Indirli *et al*. 2001, Castellano 2001, Preciado 2011 and 2015 and Preciado *et al*. 2016).

The combination of a removable prestressing system with FRP strips bonded to the masonry surface may be useful in order to wrap the structure at key internal and non-visual parts as in the case of belfries (Preciado *et al.* 2015a-c).

The stiffness of a masonry tower depends on its geometry and presence of openings, height, materials density and Young's modulus, as well as the boundary conditions (e.g., Sepe *et al.* 2008). The presence of windows and doors in masonry towers has a slight impact in terms of frequency if compared with a similar tower without openings. Preciado (2011) affirms that the slight difference in the first natural frequencies of towers with openings and without depends on the mass contribution, being stiffer the towers with openings. The material´s properties and height have a great impact on the vibration behavior of towers. Tall towers between 35-60 m are governed by a frequency domain ranging from 0.6 to 1 Hz (e.g., Slavik 2002, Ivorra and Pallares 2006, Russo *et al.* 2010). In addition, the stiffness contribution induced by adjacent buildings or façades has an impact on the dynamic response of the tower. Preciado (2011) studied the frequency domain of isolated towers and non-isolated ones taking into account the interaction with neighbor buildings by linear elastic springs of constant stiffness. The author concluded that the frequency increment is mainly observed in masonry towers with neighbor buildings, especially in the first natural frequencies represented by bending in two main directions in the range of 8-24%. Since prestressing does not add mass to the bare structure, nor large stiffened areas, it is not expected a substantial increment of frequencies. The change is more obvious in the seismic behavior studied through the capacity curves, so, the higher the compressive induced forces by prestressing, the higher the lateral strength, becoming stiffer than the bare structure without adding mass and nor changing the E modulus.

The main objectives of this Paper are the demonstration in quantitative terms of the superelastic behavior of SMA wires in pre-stressed historical masonry towers, the seismic performance contribution and changes of prestressing forces. In this study, the proposed PDs are compatible, durable and reversible, which are fundamental aspects to be taken into account for the seismic retrofitting of cultural heritage. Moreover, to conform to the fundamental requirements of structures under seismic action, the EC-8 (Eurocode 8 2004) specifies that at ultimate limit state (ULS), the capacity of the retrofitting device shall be checked in terms of strength and deformability. The level of improvement strongly depends on the level of the PF, so, the higher the force, the higher the lateral structural strength enhancement (Sperbeck 2009 and Preciado 2011). Especial careful may be taken into account when using this technique in high-rise historical masonry towers, because it may lead to a brittle failure. These massive structures are subjected to high vertical loading induced by self-weight concentrated at the base. In static conditions, an increase of the vertical loading with the post-tensioning forces may induce an exceeding of the intrinsic compressive strength, leading to a brittle failure of the complete structure by masonry crushing. Moreover, slender masonry towers may present during strong-motion EQs, large top deformation,

inducing at ultimate conditions an uncontrolled elongation of the tendons, and with this, to increasing forces that may cause masonry crushing. Therefore, an optimal post-tensioning level may be designed, due to high post-tensioning forces may lead to local damage at the anchorage zone, or a sudden brittle collapse in both static and seismic conditions. This Paper presents the investigation about how to define the level of post-tensioning force by taking care of not increasing the tower's stiffness that may cause masonry crushing. Tall masonry towers are ductile by nature; this has to be also considered when studying different prestressing levels in order to avoid a reduction of the top displacement capability.

### 3.1 Validation of the used shape memory alloy model

The most common used SMA devices for engineering purposes are made of NiTi wires, due to their relative low cost and superior behavior if compared to other conventional wire materials. The constitutive material model developed by Auricchio (1995) and Auricchio and Sacco (1997) is used to validate the superelastic behavior of SMA. The three commercial NiTi SMA wires of Table 2 are subjected to numerical tests under uniaxial tension. The numerical simulations are compared against reported experimental results by Fugazza (2003). In general, when a SMA specimen is under uniaxial tensile stresses above the austenite start stress $\sigma_s^{A\text{-}S}$, the phase transformation from austenite to martensite starts (forward transformation). At austenite finish stress $\sigma_f^{A\text{-}S}$, the phase transformation is complete. When the specimen is subjected to a high stress

Table 2 Different tendon materials under investigation

| Steel | Prestressing steel | Colddrawnwire (5–7 mm) |
|-------|-------------------|------------------------|
| FRP | Aramid FRP (AFRP) | Arapree bar (7.5 mm) |
| | | Technora bar (8 mm) |
| | Carbon FRP (CFRP) | CFCC bar (12.5 mm) |
| | | Leadline bar (7.9 mm) |
| SMA | GAC Int. | NiTi wire (0.64 × 0.46 mm) |
| | NDC Devices | NiTi wire (1.49 mm) |
| | FIP Ind. | NiTi wire (2.01 mm) |
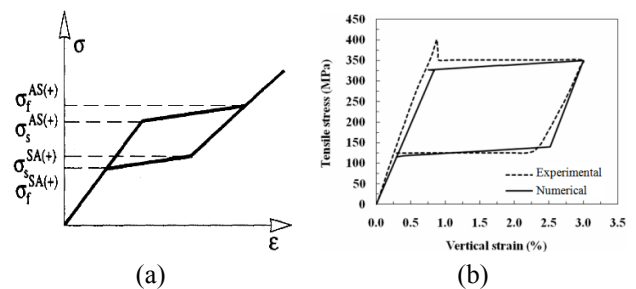


Fig. 3 NiTi SMA wires; (a) typical one-dimensional superelastic behavior (Auricchio and Sacco 1997); and (b) numerical vs experimental vertical stress-strain diagram

level such as $\sigma > \sigma_f^{A\text{-}S}$, the material exhibits the elastic behavior of the martensite phase. If unloading, the reverse transformation starts at a stress $\sigma_s^{S\text{-}A}$ and it is completed at a stress $\sigma_f^{S\text{-}A}$. The large deformation between both transformation phases leads to the formation of a hysteretic loop in the loading/unloading stress-strain diagram (see Fig. 3(a)).

The tested GAC® NiTi SMA wire has a rectangular cross section of 0.64 × 0.46 mm and a length of 5 mm. The 3D FEM model is constructed in ANSYS® with only one Solid185 element fixed at the base. This element is the recommended to simulate the superelastic SMA behavior and it is defined by eight nodes with three translational degrees of freedom at each node.

The uniaxial tension is applied under monotonically increased vertical force control until reaching the complete austenite phase transformation at a stress $\sigma_f^{A\text{-}S}$ (350 MPa). Afterwards, it is unloaded to induce the complete reverse transformation. The numerical and experimental results of the stress-strain diagram show a satisfactory agreement (Fig. 3(b)). It is worth noting that the model is able to satisfactorily capture the SMA superelasticity, maximum recoverable strain and both transformation phases.

## 4. Parametric numerical study by nonlinear static analyses

The parametric study includes different tendon material such as conventional prestressing steel, FRPs (aramid and carbon) and different NiTi SMAs. The main goal of the parametric study is the investigation of the impact on the seismic performance of different parameters such as tendon material (uniform material and combinations with segments of SMAs), different PLs, changes in tendon forces, masonry crushing and SMA superelasticity. The parametric study is based on a series of nonlinear static simulations by the pushover procedure. More than 100 nonlinear static simulations with a calculation time of about 10 hours each are carried out on a selected slender URM tower. The bare tower is subjected to a displacement based pushover analysis and presents at ULS a maximum lateral capacity of 1600 kN and a total top displacement of 265 mm. The nonlinear behavior of masonry and SMA superelasticity are simulated by including in the simulations the aforementioned material models, which are able to be included in the commercial software ANSYS®. The results are compared each other, highlighting the advantages and drawbacks of the evaluated device and prestressing forces in terms of seismic performance and observed failure modes. The external prestressing system of Fig. 4, consists of four devices vertically located and without drilling in the internal part of the tower (attached onto the bare-surface), anchored at the top and foundation.

The tendons are numerically simulated as attached to a perimetral load-distribution beam with linear-elastic behavior and the prestressing effect is simulated by means of strains, which is more effective than forces to simulate a realistic effect of tendon restoring forces. In the prestressing system of Fig. 4(a), the tendon material may be made of conventional steel, aramid fibers (AFRP) or carbon (CFRP).
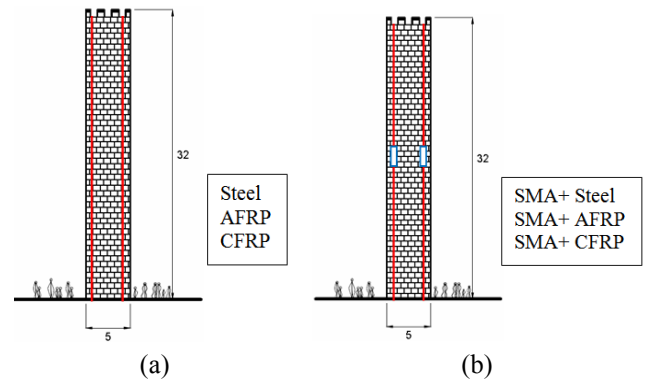


Fig. 4 Location of the reversible prestressing systems; (a) uniform devices; and (b) combined devices with segments of NiTi SMAs

Due to the high costs of SMAs, the NiTi SMAs described in Table 2 are used in small segments in combination with other tendon materials (Fig. 4(b)). The SMAs segments are located at the middle part of the tower as shown in Fig. 4(b). The used FE elements to simulate the tendons correspond to Link10 (only tension) elements with linear-elastic behavior and Solid185 elements for the SMA segments.

The total PFs are determined by taking into account different percentages of the total vertical weight: low (5%), medium (15%) and high (30%). The PDs are designed for the three PLs and reviewed in static and seismic conditions considering the mechanical properties and safety factors. Moreover, in seismic conditions, the devices are checked at the point where the structure reaches its ultimate capacity (ULS) to verify the EC-8 specifications (Eurocode 8 2004) and to assess the seismic performance, failure mechanisms and tendon restoring forces (changes in prestressing forces). Due to the tower top rotation by bending behavior, the tendons experience effects of elongation and shortening. This elongation represents an increasing of the PF and subsequently an increasing of the applied compression to the masonry. In the case of shortening, the opposite occurs.

### 4.1 Seismic analyses with low prestressing level

In this first case, a low PL is applied by taken into account a 5% of the vertical loading (0.05Fv). The total vertical loading of this tower is 18900 kN, so the total applied prestressing tensile force results in 945 kN (a precompression stress of 0.045 MPa). Four vertical PDs are considered, one in every corner of the tower with a PF each of 236.25 kN. The devices are designed/reviewed for this initial PF in static and seismic conditions. For steel, it is recommended not to exceed a 70-80% of the ultimate tensile strength, meanwhile for FRPs is of about 40% of the ultimate capacity for AFRP and 60% for CFRP due to limitations of FRPs by failing brittle. For SMA, there is no safety factor reported in literature, it is just recommended not to exceed the ultimate tensile strength of the complete austenite phase transformation ($\sigma_f^{A\text{-}S}$).

Table 3 presents the designed devices for this low PL. It is worth noting that the cross sections are over-designed

Table 3 Designed UDs and CDs for a low PL 0.05Fv

| Device | E (MPa) | A (mm²) | No. of wires/bars | $\sigma_{Acting}$ (MPa) | $\sigma_{Perm.}$ (MPa) |
|---|---|---|---|---|---|
| Steel ø = 27 mm | 210000 | 560 | 11 wires (7 mm) | 422 | 1169 |
| Arapree ø = 27 m | 62500 | 560 | 10 bars (7.5 mm) | 422 | 548 |
| Technora ø = 27 mm | 54000 | 560 | 8 bars (8 mm) | 422 | 760 |
| CFCC ø = 27 mm | 137300 | 560 | 3 bars (12.5 mm) | 422 | 1122 |
| Leadline ø = 27 mm | 150000 | 560 | 8 bars (7.9 mm) | 422 | 1350 |
| GAC® SMA ø = 56 mm | 47000 | 2500 | 7083 wires (0.64 mm) | 95 | 350 |
| NDC®SMA ø = 56 mm | 60000 | 2500 | 1078 wires (1.49 mm) | 95 | 600 |
| FIP® SMA ø = 56 mm | 80000 | 2500 | 592 wires (2.01 mm) | 95 | 670 |

due to at a first instance the changes in PFs at ULS of the tower are unknown. The vertical distribution of stresses at the tower in static conditions are in the order of 0.59 and 0.66 MPa, which are lower than the intrinsic compressive strength of 3.5 MPa. By retrofitting the tower with the low PL 0.05Fv, the concentration of compressive stresses at the bottom are checked again and are of about 0.68 MPa, which approximately corresponds to addition of the applied precompression of 0.045 MPa, being the tower stable in static conditions. This initial check in static conditions prevents a brittle collapse of the tower by masonry crushing. However, the main challenge is under seismic conditions at ULS, where the incremental vertical forces due to restoring forces may exceed the intrinsic compressive strength of masonry.

### 4.1.1 Capacity curves and failure mechanisms with low prestressing

The seismic analyses results of the bare tower and retrofitted with different devices and low PL are illustrated in Figs. 5-6. The tower presents at ULS a failure mechanism governed by bending behavior. The failure modes and plastic deformation of the retrofitted tower with UDs and CDs do not present important variations.

Due to illustrative and practical purposes, only the failure modes of the retrofitted tower with one UD (steel) and one combined (SMA+steel) are presented. The retrofitted tower with UDs reaches the ULS at a total displacement of 270 mm and presents large in-plane and out-of-plane horizontal cracks (Fig. 5(a)).

Due to symmetry of the tower, only the front view is illustrated. Conversely, the retrofitted tower with CDs reaches ultimate conditions at a displacement of 265 mm with similar horizontal cracks out of the plane as in the case of the UDs, but different height of the horizontal cracks in the plane (Fig. 5(b)). This slight different behavior of the retrofitted tower with CDs at ULS could be observed by



(a)　　　　　　　　(b)
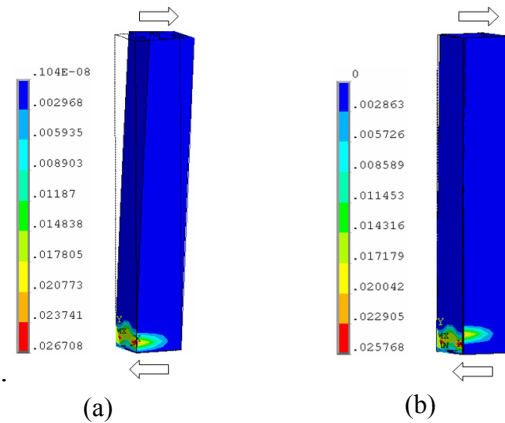
Fig. 5 Retrofitted medieval tower (0.05Fv). Principal plastic strain contours at ULS: (a) UDs at $U_H$ = 270 mm; and (b) CDs at $U_H$ = 265 mm
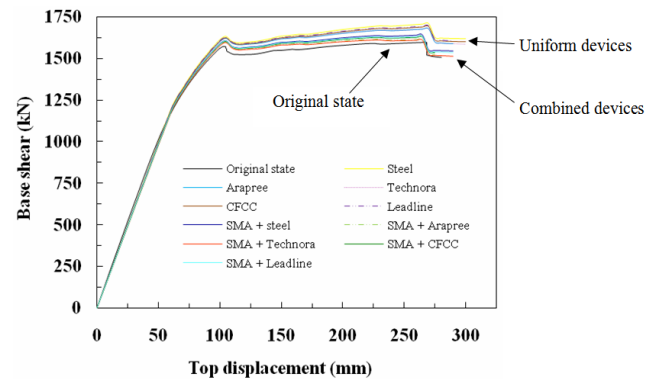


Fig. 6 Medieval tower. Comparison of capacity curves in original state and retrofitted (0.05Fv) with UDs and CDs

comparing both plastic activities and lateral displacements. The failure by masonry crushing is not presented, due to the maximum value of stress in the compressed in-plane and out-of-plane toes is in the order of 3.177 MPa for the case of the UDs and 3.149 MPa for the CDs, which are lower than the intrinsic strength (3.5 MPa). Fig. 6 illustrates the comparison of capacity curves of the bare tower and retrofitted with the UDs and CDs. It is observed that both retrofitting cases do not increase the stiffness of the tower in the linear-elastic range. The differences in lateral force and displacement are more evident in the nonlinear range, increasing both retrofitting the seismic performance. The retrofitted tower with the UDs reaches ULS for the five cases at 270 mm but different base shear, being steel the presenting more capacity (1708 kN). The CDs show a displacement of 265 mm and a lower lateral load capacity (Table 4).

### 4.1.2 Changes in forces with low prestressing

In order to verify that the ultimate capacity of the PDs is not exceeded as specified in the EC-8, the devices are checked at the point where the structure reaches the ULS. As aforementioned, in seismic conditions the tower experiences important top rotation due to its natural bending

Table 4 Seismic analysis summary of the retrofitted medieval tower (0.05Fv) at ULS

| Device | Steel | Ara. | Tech. | CFCC | Lead. |
|--------|-------|------|-------|------|-------|
| F (kN) | 1708 | 1679 | 1677 | 1694 | 1696 |
| U (mm) | 270 | 270 | 270 | 270 | 270 |
| Device | SMA + Steel | SMA + Ara. | SMA + Tech. | SMA + CFCC | SMA + Lead. |
| F (kN) | 1642 | 1614 | 1613 | 1629 | 1631 |
| U (mm) | 265 | 265 | 265 | 265 | 265 |

*Ara: Arapree; Tech: Technora; Lead: Leadline
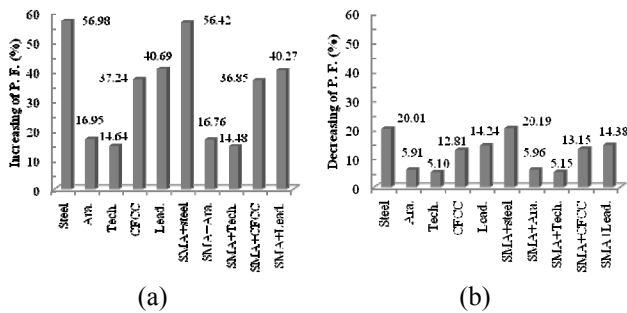


Fig. 7 Medieval tower. Changes of PFs (0.05Fv) at ULS: (a) increasing at left tendons; and (b) decreasing at right tendons

Table 5 Designed UDs and CDs for a medium PL 0.15Fv

| Device | E (MPa) | A (mm²) | No. of wires/bars | $\sigma_{Acting}$ (MPa) | $\sigma_{Perm.}$ (MPa) |
|--------|---------|---------|-------------------|-------------------------|------------------------|
| Steel ø = 46 mm | 210000 | 1680 | 33 wires (7 mm) | 422 | 1169 |
| Arapree ø = 46 mm | 62500 | 1680 | 29 bars (7.5 mm) | 422 | 548 |
| Technora ø = 46 mm | 54000 | 1680 | 25 bars (8 mm) | 422 | 760 |
| CFCC ø = 46 mm | 137300 | 1680 | 10 bars (12.5 mm) | 422 | 1122 |
| Leadline ø = 46 mm | 150000 | 1680 | 26 bars (7.9 mm) | 422 | 1350 |
| GAC® SMA ø = 67 mm | 47000 | 3500 | 9917 wires (0.64 mm) | 203 | 350 |
| NDC® SMA ø = 67 mm | 60000 | 3500 | 1509 wires (1.49 mm) | 203 | 600 |
| FIP® SMA ø = 67 mm | 80000 | 3500 | 828 wires (2.01 mm) | 203 | 670 |

behavior, leading to elongation and shortening of the tendons. Fig. 7 illustrates the changes of PFs at ULS for a low PL due to top rotation. It could be observed that the left tendons are the ones that present higher changes in PFs due to the increase in height by the flexural cracks opening. Each of the left tendons presents different force increasing depending of the E modulus of the tendon material (Table 3). Steel is the stiffer PD and Technora the less stiff. So, the higher the E modulus, the higher the changes in PFs.

Comparing the increasing in PFs of Fig. 7(a), it is worth noting a small decreasing at the CDs in the order of 1%. This is due to the different displacement at ULS (265 mm), compared to the UDs (270 mm). So, the higher the ductility, the higher the changes in PFs and plastic activity. Moreover, the localized stiffness contributed by the over-designed SMA device may explain the different crack pattern (Fig. 5) and seismic performance (see Fig. 6 and Table 4). The CDs present a lower force capacity of about 4%, and 2% of lower displacement. For this increasing in PFs at ULS, the safety of the devices is reviewed again and in any case occurs an exceedance of the design strengths ($\sigma_{Acting}$ < $\sigma_{Perm}$). Fig. 7(b) shows the decreasing of PFs at the right tendons due to the shortening. These changes are lower if compared to the presented at the elongated tendons (Fig. 7(a)) because the change in height is lower at the compressed tower's part (see the deformed shapes of Fig. 5).

### 4.2 Seismic analyses with medium prestressing level

In this second case, a medium PL is considered and corresponds to a 15% of the vertical loading (0.15Fv). The

total applied prestressing tensile force is 2835 kN (precompression of 0.135 MPa). Four PDs are applied with a post-tensioned force each of 708.75 kN. Table 5 illustrates the designed devices for this PL. The compressive stresses concentration at the base of the tower is checked again and is of about 0.74 MPa, which approximately corresponds to the addition of the applied precompression of 0.135 MPa. The tower is stable in static conditions due to the vertical stresses at the bottom are lower than the masonry strength.

### 4.2.1 Capacity curves and failure mechanisms with medium prestressing

As in the case of the low PL, the tower presents in both retrofitting cases (UDs and CDs) a failure mode governed by bending. The maximum plastic strain values in the retrofitted tower with UDs (Fig. 8(a)) are approximately
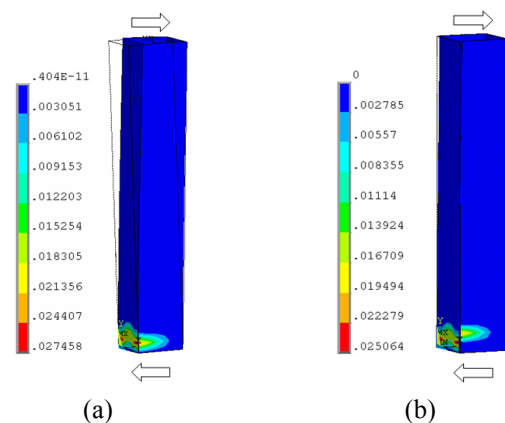


Fig. 8 Retrofitted medieval tower (0.15Fv). Principal plastic strain contours at ULS: (a) UDs at $U_H$ = 285 mm and (b) CDs at $U_H$ = 270 mm
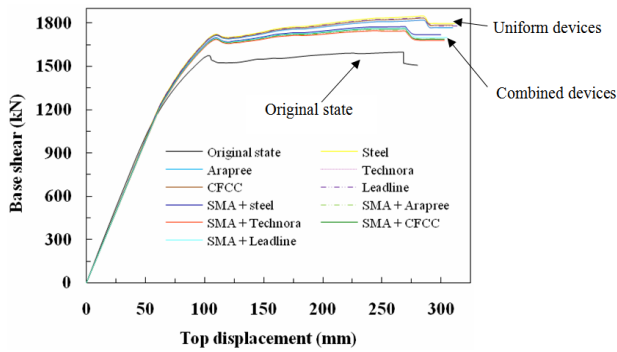
Fig. 9 Medieval tower. Comparison of capacity curves in original state and retrofitted (0.15Fv) with UDs and CDs



Fig. 10 Medieval tower. Changes of PFs (0.15Fv) at ULS: (a) increasing at left tendons; and (b) decreasing at right tendons

Table 6 Seismic analysis summary of the retrofitted medieval tower (0.15Fv) at ULS

| Device | Steel | Ara. | Tech. | CFCC | Lead. |
|---|---|---|---|---|---|
| F (kN) | 1850 | 1821 | 1820 | 1836 | 1839 |
| U (mm) | 285 | 285 | 285 | 285 | 285 |
| Device | SMA + Steel | SMA + Ara. | SMA + Tech. | SMA + CFCC | SMA + Lead. |
| F (kN) | 1776 | 1749 | 1747 | 1763 | 1765 |
| U (mm) | 270 | 270 | 270 | 270 | 270 |

*Ara: Arapree; Tech: Technora; Lead: Leadline

Table 7 Designed UDs and CDs for a high PL 0.30Fv

| Device | E (MPa) | A (mm²) | No. of wires/bars | $\sigma_{Acting}$ (MPa) | $\sigma_{Perm.}$ (MPa) |
|---|---|---|---|---|---|
| Steel ø = 65 mm | 210000 | 3360 | 65 wires (7 mm) | 422 | 1169 |
| Arapree ø = 65 mm | 62500 | 3360 | 57 bars (7.5 mm) | 422 | 548 |
| Technora ø = 65 mm | 54000 | 3360 | 50 bars (8 mm) | 422 | 760 |
| CFCC ø = 65 mm | 137300 | 3360 | 21 bars (12.5 mm) | 422 | 1122 |
| Leadline ø = 65 mm | 150000 | 3360 | 51 bars (7.9 mm) | 422 | 1350 |
| GAC® SMA ø = 91 mm | 47000 | 6500 | 18417 wires (0.64 mm) | 218 | 350 |
| NDC® SMA ø = 91 mm | 60000 | 6500 | 2802 wires (1.49 mm) | 218 | 600 |
| FIP® SMA ø = 91 mm | 80000 | 6500 | 1538 wires (2.01 mm) | 218 | 670 |

10% higher than the retrofitted with CDs (Fig. 8(b)). This is due to the tower reaches the ULS at 15 mm more displacement, which leads to a more ductile behavior and with this to a higher concentration of stresses at the base (3.342 MPa). The retrofitted tower with CDs presents compressive stresses of 3.260 MPa causing no crushing in both retrofitting cases.

It could be observed in the comparison of capacity curves that both retrofitting cases considerably improve the seismic performance of the bare tower by increasing lateral load capacity and displacement (see Fig. 9). This increasing in load-displacement allows to the structure a higher dissipation of EQ energy. The retrofitted tower with the UDs reaches an ULS for the five cases at a displacement of 285 mm but presents different lateral force, being steel the one that shows better performance (1850 kN). The CDs present lower displacement (270 mm) and force capacity due to the concentration of stresses induced by the localized SMA stiffness (see Table 6).

### 4.2.2 Changes in forces with medium prestressing

For this intermediate PL the changes of PFs are analyzed at ULS to verify that the ultimate capacity of the devices is not exceeded, as well as the magnitude of the transmitted compressive stresses to the masonry. The changes of PFs at left and right tendons for the two retrofitting cases and all the devices are illustrated in Fig. 10. It is worth noting that in the case of the low PL the changes of PFs depend on the E modulus of the device, location with respect to the seismic loading (left or right) and the

resulting bending top rotation. Moreover, the changes of PFs have reduced about 65% if compared to the low level, because the top rotation is reduced by the increased precompression level. The safety analysis of the devices indicates that in any case the design strengths are exceeded.

### 4.3 Seismic analyses with high prestressing level

In this final case, a high precompression level is taken into account corresponding to a 30% of the vertical loading (0.30Fv). A post-tensioned force of about 1417.5 kN is applied to each device (a total force of 5670 kN and a level of precompression of 0.269 MPa (see Table 7). In static conditions, the concentration of compressive stresses at the bottom of the tower is in the order of 0.80 MPa, being lower than the masonry strength. The cross sections are proposed with a certain level of over-design to withstand this high PL in static conditions including a safety factor due to the possible changes in PFs at seismic ULS.

(a)            (b)
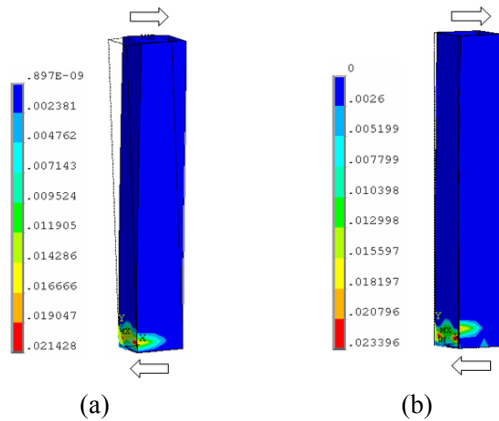
Fig. 11 Retrofitted medieval tower (0.30Fv). Principal plastic strain contours at ULS: (a) UDs at $U_H$ = 260 mm and (b) CDs at $U_H$ = 275 mm
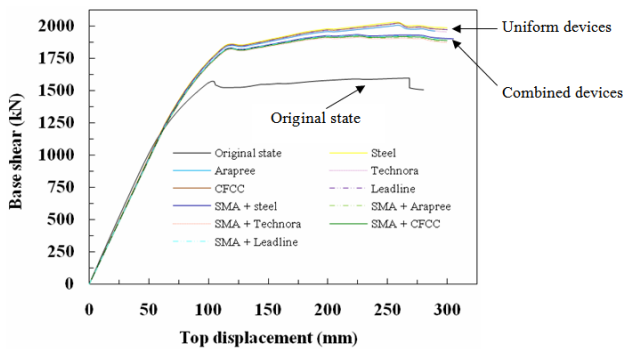


Fig. 12 Medieval tower. Comparison of capacity curves in original state and retrofitted (0.30Fv) with UDs and CDs

### 4.3.1 Capacity curves and failure mechanisms with high prestressing

As in the two previous PLs, the tower presents in both retrofitting cases a flexural failure mode with the presence of similar out-of-plane horizontal cracks (see Fig. 11).

In this case, the opposite of the low and medium PLs occurs regarding plasticity and displacement capability at ULS. The maximum plastic strain values by the UDs (Fig. 11(a)) are approximately 8.5% lower than the presented by the CDs (Fig. 11(b)), showing 15 mm less displacement. This increase in displacement by the CDs leads to a stress concentration at the toes of 3.388 MPa, becoming evident the early formation of a slight vertical cracking (see Fig. 11(b)) because the compressive ultimate strength of masonry is almost reached.

Conversely, the retrofitted tower with UDs presents compressive stresses of 3.344 MPa with no vertical cracking. A possible reason to explain this contrast in displacement could be related to the precompression level and high concentration of stresses at the SMA near to the austenite start stress. The linear behavior of the tower is substantially increased, presenting the start of the nonlinear behavior at a lateral load of about 1450 kN and a displacement of 75 mm (see Fig. 12). The UDs permit to improve in a better way as in the two first PLs the lateral force capacity but in contrast a 15 mm displacement

Table 8 Seismic analysis summary of the retrofitted medieval tower (0.30Fv) at ULS

| Device | Steel | Ara. | Tech. | CFCC | Lead. |
|---|---|---|---|---|---|
| F (kN) | 2026 | 2009 | 2008 | 2021 | 2023 |
| U (mm) | 260 | 260 | 260 | 260 | 260 |
| Device | SMA + Steel | SMA + Ara. | SMA + Tech. | SMA + CFCC | SMA + Lead. |
| F (kN) | 1931 | 1907 | 1906 | 1919 | 1921 |
| U (mm) | 275 | 275 | 275 | 275 | 275 |

*Ara: Arapree; Tech: Technora; Lead: Leadline



(a)           (b)
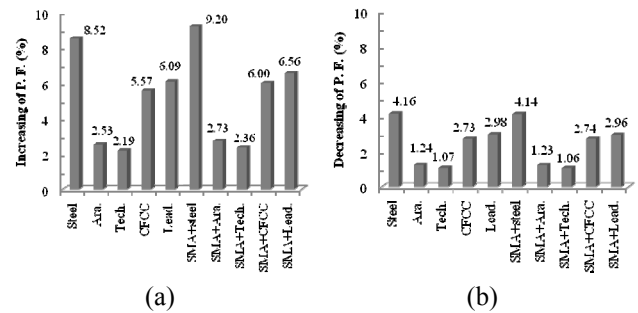
Fig. 13 Medieval tower. Changes of PFs (0.30Fv) at ULS: (a) increasing at left tendons; and (b) decreasing at right tendons

reduction. In both retrofitting cases, the tower presents a different post-peak behavior after reaching the ULS, with a more stable failure in comparison to previous PLs (see Table 8).

### 4.3.2 Changes in forces with high prestressing

The reduced top rotation of the masonry tower is due to the high level of precompression, which is also reflected in the changes of prestressing forces in the tendons (see Fig. 13). By comparing the changes of PFs at the left tendons with the low PL, there is a reduction in the order of 85%, and 57% in comparison to the medium PL. In any case, the design strength of the tendons is exceeded.

## 5. Seismic analyses with SMA induced superelasticity

In the former analyses with different PLs no especial behavior was observed in the CDs with SMA in terms of changes of PFs and seismic performance contribution. It was observed a lower lateral force and displacement contribution if compared to the uniform devices with no SMA. This was related to the contributed localized stiffness by the SMA device. This was also reflected by slight differences in the changes of PFs. In the high PL, the CDs allowed obtaining more displacement and higher changes in tendon forces than the UDs, but in contrast, presented lower lateral force contribution as in former PLs. However, in both retrofitting cases, the seismic performance of the tower was successfully enhanced. Unfortunately, it was not observed the superelastic behavior of SMA which is

characterized for keeping the PFs constant. This is due to the post-tensioned forces in static conditions and at ULS did not reach the SMA austenite start stress ($\sigma_s^{A-S}$). This led to a similar linear stress-strain behavior of conventional materials by the over-designed SMA device.

In order to observe the induced SMA superelasticity behavior, the prestressing force must be at the austenite stress level in order to reach the phase transformation with the induced lateral displacements. One main issue is to keep the applied prestressing force constant in static conditions in order to reach the transformation phase. This section aims at inducing the SMA superelasticity to quantitatively verify its contribution in the seismic performance of the tower and in the changes of PFs. The three levels of prestressing (low, medium and high) are studied through nonlinear pushover analyses. For the seismic analysis with SMA induced super-elasticity, the NDC® NiTi wire is selected due to its larger strain capability (8%) and low E modulus in comparison to the FIP® and the other SMAs (Table 2).

The stress-induced martensite (SIM) transformation is aimed at designing the cross section of the SMA device for the initial PF in static conditions at the austenite start stress ($\sigma_s^{A-S}$ = 520 MPa). Furthermore, by the increasing of the post-tensioning force at ULS to try to reach the forward transformation branch up to the austenite final stress ($\sigma_f^{A-S}$ = 600 MPa) at a strain of 8%. If the tensile stresses continue instead of following the unloading path, the large deformation could lead to the failure of the SMA as observed in the experimental tests of Zurbitu *et al*. (2009). By comparing the austenite start and final stresses of the selected NiTi wire for the seismic analysis with induced superelasticity, it could be observed that the allowed stress increase is in the order of 15.4% (80 MPa). Due to this restriction, only the devices that showed in the three PLs changes of PFs lower than this percentage are selected for the investigations with SIM transformation (Figs. 7, 10 and 13). Table 9 illustrates the selected stiffer and weaker

Table 9 Designed combined devices for the stress-induced martensite transformation

| P. L. | Device | A (mm$^2$) | No. of wires/bars | $\sigma_{Acting}$ (MPa) | $\sigma_{Perm.}$ (MPa) |
|---|---|---|---|---|---|
| Low 0.05Fv 945 kN | Tech. ø = 27 mm | 560 | 8 bars (8 m) | 422 | 760 |
| | SMA ø = 24 mm | 454 | 195 wires (1.4 9mm) | 520 | 600 |
| Medium 0.15Fv 2835 kN | Tech. ø = 46 mm | 1680 | 25 bars (8 mm) | 422 | 760 |
| | SMA ø = 42 mm | 1363 | 586 wires (1.49 mm) | 520 | 600 |
| High 0.30Fv 5670 kN | Tech. ø = 65 mm | 3360 | 50 bars (8 mm) | 422 | 760 |
| | Steel ø = 65 mm | 3360 | 65 wires (7 m) | 422 | 1169 |
| | SMA ø = 59 mm | 2726 | 1172 wires (1.49 mm) | 520 | 600 |

*P.L: Prestressing level; Tech: Technora
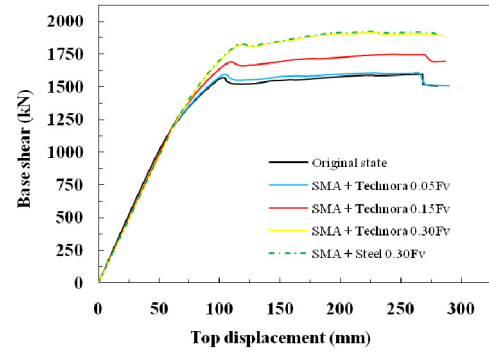


Fig. 14 Medieval tower. Comparison of capacity curves in original state and retrofitted with SMA induced superelasticity

tendon materials (steel and Technora) in combination with SMAs and their respective cross sections and PFs.

By comparing the capacity curves of the combined devices subjected to the three PLs of Figs. 6, 9 and 12, it could be observed that the current SIM transformation of SMA devices of Fig. 14 has no impact in a further improvement of the lateral load and displacement capacity as the observed without transformation. The tower presents ultimate conditions at the same displacements with minimum variations in the lateral forces (less than 1%). This trend is also reflected in the failure modes. The tower fails as well for bending and presents the same crack patterns as former PLs with minimum variations (about 1%) in the plastic activity (Figs. 5, 8 and 11). The maximum values of stress at the compressed toes are almost the same as well.

The decreasing of forces at the right tendons with the induced transformation (Fig. 15(b)) are similar than those observed without it (Figs. 7(b), 10(b) and 13(b)). The impact is observed in the elongated left tendons (Fig. 15(a)), with a substantial reduction of the increasing of forces. For the case of the combined SMA with Technora (SMA+Technora) and a low PL, the reduction at left tendons is of about 47.10%. In the medium level (SMA+ Technora) a reduction of about 13.75% is achieved and 5.08% in the high level. Conversely, a contrast in the combined SMA+steel and high PL is observed, with a reduction in the order of 26.20%. This variation is due to the high E modulus of steel in comparison to that of the
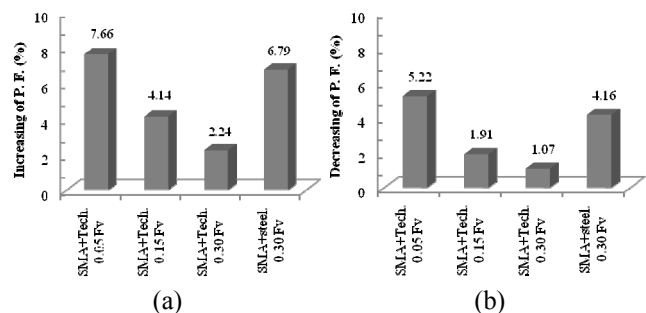


Fig. 15 Medieval tower. Changes of PFs at ULS with SMA induced superelasticity: (a) increasing at left tendons; and (b) decreasing at right tendons

Technora FRP. It is worth noting in Fig. 15(a) that the increasing of PFs in all cases is lower than the allowed increase in stress/force of 15.4% (80 MPa).

## 6. Summary of findings

Following paragraphs are aimed at summarizing the main findings on the seismic nonlinear analyses on the selected masonry tower in original state and retrofitted with different prestressing levels and devices (with variations in tendon material and combinations):

*Low prestressing level:* The tower retrofitted with steel showed more force capacity (1708 kN). The CDs showed 3.52% less plastic deformation due to the 5 mm of less displacement if compared to the UDs. Both cases enhanced the tower's seismic performance (CDs: force and UDs: force and displacement). At ULS the failure by masonry crushing was not observed. Left tendons showed higher changes in PFs due to the increase in height by the flexural cracks opening. The different increasing of PFs depended on the E modulus of the tendon material. The over-designed SMA device induced at the masonry tower localized stiffness which may be related to the different crack pattern and seismic performance between the UDs and CDs. The CDs showed lower lateral load capacities (4%) and displacement (2%). At ULS, the tower experienced important top rotation by natural bending behavior. The cracks opening led to the elongation of the left tendons and this considerably increased the PFs and the compression to the masonry. There was no device failure due to the over-designed cross sections.

*Medium prestressing level:* As in the low PL, the tower failed by bending and same crack pattern. The retrofitted tower with UD reached an ULS for the five cases at 285 mm but at different lateral force, being steel the one that presented better performance (1850 kN). The CDs presented 270 mm and lower lateral force by the SMA stiffness contribution. The plasticity at the retrofitted tower with UDs was 10% higher than with CDs, due to the 15 mm of more displacement at ULS. This led to a more ductile behavior and concentration of stresses at the compressed toes (3.342 MPa). The tower with CDs showed high compressive stresses (3.260 MPa), with no crushing (intrinsic strength of 3.5 MPa). The enhancement in terms of lateral force and displacement was obvious in the nonlinear range. In this PL the changes of PFs reduced about 65% in comparison to the low level due to the triple level of precompression. By comparing the increasing of PFs with UDs and CDs at this medium level, it was observed a decreasing of 5% on the CDs due to the SMA localized stiffness.

*High prestressing level:* The maximum plastic strains values with the UDs were 8.5% lower than with CDs and presented 15 mm less displacement. The high PL and increase in displacement with CDs led to a concentration of stresses at the compressed toes of 3.388 MPa with the formation of slight vertical cracking because of the compressive strength was almost reached. The tower with UDs presented compressive stresses of 3.344 MPa with no

vertical cracking. The start of the nonlinear behavior was observed at 1450 kN and 75 mm. The UDs improved in a better way as in the two first PLs the lateral force, but in contrast 15 mm of less displacement. The CDs presented lower force enhancement compared to the UDs but more displacement. The SMA was near to the austenite start stress, behaving less stiff than former PLs. In both retrofitting cases, the tower showed different post-peak behavior, failing more stable if compared to former PLs. The changes at left tendons in comparison to the low level decreased 85% and 57% in comparison to the medium PL.

*SMA induced superelasticity:* The SMA superelastic behavior which characterizes for keeping the PF constant was not observed through the parametric study. This was due to the post-tensioned forces in static conditions and at ULS did not reach the SMA austenite start stress because the over-designed cross-sections, behaving similar to conventional materials. The martensite transformation permitted to observe the SMA superelasticity with the increasing of PFs at ULS by reaching the forward transformation branch and without exceeding the austenite final stress leading to its failure. In the seismic analyses, the SIM transformation of SMA devices had no impact in further enhancement of the lateral load and displacement capacity. The decreasing of forces at right tendons with the transformation were similar than without it. The impact was observed in the elongated left tendons with a substantial reduction of the increasing of PFs: SMA+Technora and low PL reduced 47.10%, medium PL 13.75% and high PL 5.08%. SMA+steel and high PL showed 26.20% of reduction. In all cases, the increasing of PFs were lower than the allowed increasing rate (15.4%) of the used SMA device.

## 7. Conclusions

The capability of the applied model to simulate the superelastic behavior of SMA was validated with reported experiments, showing a very good agreement. The inclusion of the SMA material model in commercial software represents a practical tool for the simulation of experimental and numerical tests at a different scale levels from a simple wire to pre-stressing devices. An extensive parametric study on a selected slender historical masonry tower was carried out based on more than 100 nonlinear static simulations by following a displacement-based pushover technique. The parametric evaluation was objected at investigating the impact on the seismic performance of different parameters as tendon material, prestressing level, tendon force changes and SMA superelasticity. The last did not show upgrading of seismic performance due to the small SMA contribution by the device size and vertical location. To observe the SMA superelasticity behavior, the prestressing force must be at the austenite stress level to reach the phase transformation with the top displacements of the tower. If the material is in austenite phase behaves as a conventional one. The SIM transformation in vertical prestressing has only impact in keeping the applied forces with lower variations than other materials in low and medium PLs. In real applications of SMA tendons, the main issue is to keep

the applied prestressing force constant in static conditions in order to reach the transformation phase. This becomes unpractical because SMA wires are temperature dependent, becoming very difficult the calibration of prestressing forces. Tendon force control is even more complex in earthquake conditions, where the structure may reach large top displacements. However, more research is suggested regarding the use of SMA tendons for the seismic retrofitting of towers with large belfries and compact structures governed by shear failure.

In the present study, the Technora AFRP showed good performance in force and displacement enhancement with low changes in tendon forces because of its low E modulus, which is favorable to interact with old masonry. Especial attention is suggested when using high prestressing levels due to this could generate brittle failure by masonry crushing. The level of enhancement mainly depends on the applied normal forces and the tendon material as observed through the three studied prestressing levels. The higher the post-tensioning loads, the higher the reached lateral horizontal force. This effect occurs due to the incremental normal forces enhance the resistance to lateral loading of the structure. In real structures, this effect may be interpreted as a reduction of the crack opening, and thus the increasing resistance. In contrast, the obtained ultimate lateral top displacement may reduce due to the increasing of stiffness induced by high vertical prestressing levels. The reduction in crack opening reduces the natural ductile behavior of tall and heavy masonry towers because these structures dissipate most of the earthquake energy by a closing and opening effect of new and existing cracks, mainly horizontal ones induced by flexion. Tall masonry towers are massive structures subjected to high concentration of stresses at the bottom part, in addition of the degradation of the material and ambient vibration induced by traffic and wind, the intrinsic strength may be exceeded and fail brittle in a sudden way. The practical engineer must take special care in not to exceed the intrinsic strength of masonry towers by the addition of post-tensioning systems in static and ultimate seismic conditions. Therefore, it is strongly recommended a detailed diagnosis of the tower by experimental in-situ and laboratory tests including the historical analysis of damages and restorations as well as reliable numerical analyses with suitable material models and effective tools.

In the low level, the uniform devices showed better performance than the SMA, being steel the tendon material that allowed higher lateral force capacity but in contrast higher changes in forces due to its high E modulus. Technora presented a slight reduction in force capacity compared to steel, but much lower force changes by its low E modulus. In the medium level, the uniform devices showed a better performance than in the high level. In high prestressing levels, both Technora and combined SMA+Technora showed substantial enhancement and a more stable post-peak behavior than other devices. Technora FRP device allowed higher force capacity but lower displacement than SMA+Technora. Medium and high prestressing levels successfully enhanced force capacity and confinement of towers failing by pure bending. The

capacity curves were helpful to validate the seismic performance enhancement of the retrofitted tower against the bare one in terms of force and displacement. High prestressing levels by taking into account the 30% of the total vertical loading are not recommended because it induces concentration of stresses at the anchorages and may generate a brittle sudden collapse by masonry crushing even in static conditions. In the presented nonlinear seismic investigations, the retrofitted tower with this high level of prestressing did not present a huge impact on the results, in contrast the tower almost failed by crushing. Taking into account the performance based design philosophy where displacement enhancement is fundamental in retrofitted structures for energy dissipation, the medium prestressing level (0.15Fv) is the optimal for seismic performance upgrading. This intermediate prestressing level presented more displacement enhancement than the high level, and also avoids the masonry crushing even in masonry towers with a degraded intrinsic resistance throughout the years. The parametric study permitted to develop a methodology for the seismic vulnerability reduction of historical masonry towers by means of vertical external prestressing. It is worth noting that the approach was developed through historical slender URM structures presenting failure modes governed by flexion. Therefore no great impact was observed in displacement enhancement due to these structures are ductile by nature. The main challenge is focused on bell-towers with large openings at belfry, which normally fail brittle by a concentration of shear stresses at this failure point. For that purpose, the authors of this paper recommend to study the behavior of shear governed structures by the use of FRP tendons and a medium prestressing level, which may be calculated by following the presented methodology.

## References

Ascione, L., Feo, L. and Fraternali, F. (2005), "Load carrying capacity of 2D FRP/strengthened masonry structures", *Comp. Part B: Eng.*, **36**(8), 619-626.

Auricchio, F. (1995), "Shape memory alloys: micromechanics, macromodeling and numerical simulations", Ph.D. Dissertation; University of California at Berkeley, CA, USA.

Auricchio, F. and Sacco, E. (1997), "A one-dimensional model for superelastic shape-memory alloys with different elastic properties between martensite and austenite", *Int. J. Non-Lin. Mech.*, **32**, 1101-1114.

Bansal, P., Sharma, R. and Mehta, A. (2016), "Retrofitting of RC girders using pre-stressed CFRP sheets", *Steel Compos. Struct., Int. J.*, **20**(4), 833-849.

Barbieri, G., Biolzi, L., Bocciarelli, M., Fregonese, L. and Frigeri, A. (2013), "Assessing the seismic vulnerability of a historical building", *Eng. Struct.*, **57**, 523-535.

Binda, L. (2008), *Learning From Failure: Long-Term Behaviour of Heavy Masonry Structures*, WIT Press, GB; Polytechnic of Milano, Italy.

Binda, L., Gatti, G., Mangano, G., Poggi, C. and Sacchi-Landriani, G. (1992), "The collapse of the civic tower of Pavia: A survey of the materials and structure", *Masonry Int.*, 11-20.

Calderini, C. and Lagomarsino, S. (2006), "A micromechanical inelastic model for historical masonry", *Earthq. Eng.*, **10**(4), 453-479.

Castellano, M.G. (2001), "Innovative technologies for earthquake protection of architectural heritage", *Proceedings of the International Millennium Congress: More than two thousand years in the history of Architecture*, UNESCO-ICOMOS, Paris, France.

D'Ambrisi, A., Focacci, F. and Caporale, A. (2013a), "Strengthening of masonry-unreinforced concrete railway bridges with PBO-FRCM materials", *Comp. Struct.*, **102**, 193-204.

D'Ambrisi, A., Feo, L. and Focacci, F. (2013b), "Experimental and analytical investigation on bond between Carbon-FRCM materials and masonry", *Comp.Struct.*, **46**, 15-20.

Eurocode 8 (2004), Design of structures for earthquake resistance - Part 1: General rules, seismic actions and rules for buildings; European Standard.

Fedele, R., Scaioni, M., Barazzetti, L., Rosati, G. and Biolzi, L. (2014), "Delamination tests on CFRP-reinforced masonry pillars: optical monitoring and mechanical modeling", *Cement Concrete Compos.*, **45**, 243-254.

Foraboschi, P. (2013), "Church of San Giuliano di Puglia: seismic repair and upgrading", *Eng. Fail. Anal.*, **33**, 281-314.

Foraboschi, P. (2015), "Analytical model to predict the lifetime of concrete members externally reinforced with FRP", *Theoret. Appl. Fract. Mech.*, **75**(1), 137-145.

Foraboschi, P. (2016a), "The central role played by structural design in enabling the construction of buildings that advanced and revolutionized architecture", *Constr. Build. Mat.*, **114**, 956-976.

Foraboschi, P. (2016b), "Effectiveness of novel methods to increase the FRP-masonry bond capacity", *Comp. Part B: Eng.*, **107**, 214-232.

Foraboschi, P. and Vanin, A. (2013), "New methods for bonding FRP strips onto masonry structures: Experimental results and analytical evaluations", *Compos.: Mech., Comput.,Applic., An Int. J.*, **4**(1), 1-23.

Fugazza, D. (2003), "Shape-memory alloy devices in earthquake engineering: Mechanical properties, constitutive modeling and numerical simulations", Master Thesis; University of Pavia, Italy.

Gambarotta, L. and Lagomarsino, S. (1997), "Damage models for the seismic response of brick masonry shear walls", Part I and II. *Earthq. Eng. Struct. Mech.*, **26**, 441-462.

Ganz, H.R. (1990), "Post-tensioned masonry structures: Properties of masonry design considerations post-tensioning system for masonry structures applications", *VSL Report Series No. 2*, Berne, Switzerland.

Ganz, H.R. (2002), "Post-tensioned masonry around the world", *Proceedings of the first annual Conference of the Post-tensioning Institute*, San Antonio, TX, USA.

GES (1993), Technical opinion about the collapse of the bell tower of St. Maria Magdalena in Goch, Germany; Gantert Engineering Studio.

Hadji, L., Daouadji, T., Meziane, M. and Bedia, E. (2016), "Analyze of the interfacial stress in reinforced concrete beams strengthened with externally bonded CFRP plate", *Steel Compos. Struct., Int. J.*, **20**(2), 413-429.

Indirli, M., Castellano, M.G., Clemente, P. and Martelli, A. (2001), "Demo-application of shape memory alloy devices: The rehabilitation of the S. Giorgio church bell-tower", *Proceedings of SPIE, Smart Structures and Materials*.

Ivorra, S. and Pallares, F.J. (2006), "Dynamic investigations on a masonry bell tower", *Eng. Struct.*, **28**, 660-667.

Macchi, G. (1993), "Monitoring medieval structures in Pavia", *Structural Engineering International*, I/93.

Muciaccia, G. and Biolzi, L. (2012), "Thermal degradation of fiber reinforced extruded materials", *Fire Safety J.*, **49**(4), 89-99.

Panjehpour, M., Abang-Ali, A.A. and Aziz, F. (2014), "Energy absorption of reinforced concrete deep beams strengthened with CFRP sheet", *Steel Compos. Struct., Int. J.*, **16**(5), 481-489.

Park, J.W. and Yoo, J.H. (2015), "Flexural and compression behavior for steel structures strengthened with carbon fiber reinforced polymers (CFRPs) sheet", *Steel Compos. Struct., Int. J.*, **19**(2), 441-465.

Preciado, A. (2011), "Seismic vulnerability reduction of historical masonry towers by external prestressing devices", Ph.D. Dissertation; Technical University of Braunschweig, Germany and University of Florence, Italy.

Preciado, A. (2015), "Seismic vulnerability and failure modes simulation of ancient masonry towers by validated virtual finite element models", *Eng. Fail. Anal.*, **57**, 72-87.

Preciado, A. and Orduña, A. (2014), "A correlation between damage and intensity on old masonry churches in Colima, Mexico by the 2003 M7.5 earthquake", *Case Stud. Struct. Eng.*, **2**, 1-8.

Preciado, A., Lester, J., Ingham, J.M., Pender, M. and Wang, G. (2014), "Performance of the Christchurch, New Zealand Cathedral during the M7.1 2010 Canterbury earthquake", *Proceedings of the 9th International Conference on Structural Analysis of Historical Constructions* (*SAHC*), *Topic 11*, *Paper 02*, Mexico City, Mexico, October.

Preciado, A., Orduña, A., Bartoli, G. and Budelmann, H. (2015a), "Façade seismic failure simulation of an old Cathedral in Colima, Mexico by 3D Limit Analysis and nonlinear Finite Element Method". *Eng. Fail. Anal.*, **49**, 20-30.

Preciado, A., Bartoli, G. and Budelmann, H. (2015b), "Fundamental aspects on the seismic vulnerability of ancient masonry towers and retrofitting techniques", *Earthq. Struct., Int. J.*, **9**(2), 339-352.

Preciado, A., Bartoli, G. and Budelmann, H. (2015c), "The use of prestressing through time as seismic retrofitting of historical masonry constructions: Past, present and future perspective". *Revista Ciencia Ergo-Sum*, **22**(3), 242-252.

Preciado, A., Sperbeck, S.T. and Ramirez-Gaytan, A. (2016), "Seismic vulnerability enhancement of medieval and masonry bell towers externally prestressed with unbonded smart tendons", *Eng.Struct.*, **122**, 50-61.

Preciado, A., Bartoli, G. and Ramirez-Gaytan, A. (2017), "Earthquake protection of the Torre Grossa medieval tower of San Gimignano, Italy by vertical external prestressing", *Eng. Fail. Anal.*, **71**, 31-42.

Raijmakers, T.M.J. and Vermeltfoort, A.T. (1992), Deformation controlled tests in masonry shear walls (in Dutch); Report B-92-1156, TNO-Bouw, Delft, The Netherlands.

Russo, G., Bergamo, O., Damiani, L. and Lugato, D. (2010), "Experimental analysis of the Saint Andrea masonry bell tower in Venice: A new method for the determination of tower global young´s modulus E", *Eng. Struct.*, **32**(2), 353-360.

Sepe, V., Speranza, E. and Viskovic, A. (2008), "A method for large-scale vulnerability assessment of historic towers", *Struct. Control Health Monit.*, **15**, 389-415.

Slavik, M. (2002), "Assessment of bell towers in Saxony", *Proceedings of the 4th International Conference on Structural Dynamics* (*EURODYN*), Munich, Germany, September.

Sperbeck, S.T. (2009), "Seismic risk assessment of masonry walls and risk reduction by means of prestressing", Ph.D. Dissertation; Technical University of Braunschweig, Germany and University of Florence, Italy.

Stavroulaki, M.E., Bartoli, G., Betti, M. and Stavrolakis, G.E. (2009), "Strengthening of masonry using metal reinforcement: A parametric numerical investigation", *Proceedings of the International Conference on Protection of Historical Buildings* (*PROHITECH*), Rome, Italy, June.

Urban, M. (2007), "Earthquake risk assessment of historical structures", Ph.D. Dissertation; Technical University of Braunschweig, Germany and University of Florence, Italy.

Van der Pluijm, R. and Vermeltfoort, A.T. (1991), Deformation controlled tension and compression tests in units, mortar and masonry (in Dutch); Report B-91-0561, The Netherlands.

Vermeltfoort, A.T. and Raijmakers, T.M.J. (1993), Deformation controlled tests in masonry shear walls, Part 2 (in Dutch), Report TUE/BKO/93.08, Eindhoven University of Technology, The Netherlands.

Zurbitu, J., Castillo, G., Urrutibeascoa, I. and Aurrekoetxea, J. (2009), "Low-energy tensile-impact behavior of superelastic NiTi shape memory alloy wires", *Mech. Mat.*, **41**, 1050-1058.

*CC*